BRAIN
A JOURNAL OF NEUROLOGY

Phenotypic and molecular insights into spinal muscular atrophy due to mutations in *BICD2*

Alexander M. Rossor,[1,]* Emily C. Oates,[2,3,]* Hannah K. Salter,[4] Yang Liu,[4]
Sinead M. Murphy,[5,6] Rebecca Schule,[7,8] Michael A. Gonzalez,[8] Mariacristina Scoto,[9]
Rahul Phadke,[1] Caroline A. Sewry,[9] Henry Houlden,[1] Albena Jordanova,[10,11,12]
Iyailo Tournev,[13,14] Teodora Chamova,[13] Ivan Litvinenko,[15] Stephan Zuchner,[8]
David N. Herrmann,[16] Julian Blake,[17,18] Janet E. Sowden,[19] Gyuda Acsadi,[20]
Michael L. Rodriguez,[21,22] Manoj P. Menezes,[2,3] Nigel F. Clarke,[2,3]
Michaela Auer Grumbach,[23] Simon L. Bullock,[4] Francesco Muntoni,[1,9] Mary M. Reilly[1,†] and
Kathryn N. North[2,3,24,25,†]

*,†These authors contributed equally to this work.

Spinal muscular atrophy is a disorder of lower motor neurons, most commonly caused by recessive mutations in *SMN1* on chromosome 5q. Cases without *SMN1* mutations are subclassified according to phenotype. Spinal muscular atrophy, lower extremity-predominant, is characterized by lower limb muscle weakness and wasting, associated with reduced numbers of lumbar motor neurons and is caused by mutations in *DYNC1H1*, which encodes a microtubule motor protein in the dynein-dynactin complex and one of its cargo adaptors, BICD2. We have now identified 32 patients with *BICD2* mutations from nine different families, providing detailed insights into the clinical phenotype and natural history of BICD2 disease. BICD2 spinal muscular atrophy, lower extremity predominant most commonly presents with delayed motor milestones and ankle contractures. Additional features at presentation include arthrogryposis and congenital dislocation of the hips. In all affected individuals, weakness and wasting is lower-limb predominant, and typically involves both proximal and distal muscle groups. There is no evidence of sensory nerve involvement. Upper motor neuron signs are a prominent feature in a subset of individuals, including one family with exclusively adult-onset upper motor neuron features, consistent with a diagnosis of hereditary spastic paraplegia. In all cohort members, lower motor neuron features were static or only slowly progressive, and the majority remained ambulant throughout life. Muscle MRI in six individuals showed a common pattern of muscle involvement with fat deposition in most thigh muscles, but sparing of the adductors and semitendinosus. Muscle pathology findings were highly variable and included pseudomyopathic features, neuropathic features, and minimal change. The six causative mutations, including one not previously reported, result in amino acid changes within all three coiled-coil domains of the BICD2 protein, and include a possible 'hot spot' mutation, p.Ser107Leu present in four families. We used the recently solved crystal structure of a highly conserved region of the *Drosophila* orthologue of BICD2 to further-explore how the p.Glu774Gly substitution inhibits the binding of BICD2 to Rab6. Overall, the features of BICD2 spinal muscular atrophy, lower extremity predominant are consistent with a pathological process that preferentially affects lumbar lower motor neurons, with or without additional upper motor neuron involvement. Defining the phenotypic features in this, the largest BICD2 disease cohort reported to date, will facilitate focused genetic testing and filtering of next generation sequencing-derived variants in cases with similar features.

1 MRC Centre for Neuromuscular Diseases, UCL Institute of Neurology, London, WC1N 3BG, UK
2 Institute for Neuroscience and Muscle Research, Children's Hospital at Westmead, New South Wales, 2145, Australia
3 Discipline of Paediatrics and Child Health, Faculty of Medicine, The University of Sydney, Sydney, New South Wales, 2006, Australia
4 Cell Biology Division, MRC Laboratory of Molecular Biology, Cambridge, CB2 0QH, UK
5 Department of Neurology, Adelaide and Meath Hospitals Incorporating the National Children's Hospital, Tallaght, Dublin, Ireland
6 Academic Unit of Neurology, Trinity College Dublin, Ireland
7 Hertie Institute for Clinical Brain Research and Centre for Neurology, Department of Neurodegenerative Disease, University of Tübingen and the German Research Centre for Neurodegenerative Diseases (DZNE), Tübingen, Germany
8 Dr. John T. Macdonald Foundation Department of Human Genetics and John P. Hussman Institute for Human Genomics, University of Miami Miller School of Medicine, Miami, Florida, 33136, USA
9 Dubowitz Neuromuscular Centre, UCL Institute of Child Health, London, WC1N 1EH, UK
10 Molecular Neurogenomics Group, Department of Molecular Genetics, VIB, Antwerp 2610, Belgium
11 Neurogenetics Laboratory, Institute Born-Bunge, University of Antwerp, Antwerp 2610, Belgium
12 Department of Medical Chemistry and Biochemistry, Molecular Medicine Centre, Medical University-Sofia, Sofia 1431, Bulgaria
13 Department of Neurology, Medical University-Sofia, Sofia 1000, Bulgaria
14 Department of Cognitive Science and Psychology, New Bulgarian University, Sofia
15 Clinic of Child Neurology, Department of Paediatrics, Medical University-Sofia, Sofia 1000, Bulgaria
16 University of Rochester Medical Centre, Departments of Neurology and Pathology, Rochester, NY, 14642, USA
17 Department of Clinical Neurophysiology, The National Hospital for Neurology and Neurosurgery and Department of Molecular Neuroscience, UCL Institute of Neurology, London, UK
18 Department of Clinical Neurophysiology, Norfolk and Norwich University Hospital, UK
19 University of Rochester Medical Centre, Department of Neurology, Rochester, NY, 14642, USA
20 Connecticut Children's Medical Centre, Department of Neurology, Hartford Connecticut, 06106, USA
21 Department of Forensic Medicine, Sydney Local Health District, New South Wales, 2037, Australia
22 Discipline of Pathology, Sydney Medical School, The University of Sydney, Sydney, New South Wales, 2006, Australia
23 Division of Orthopaedics, Medical University of Vienna, Währinger Gürtel 18-20, A-1090 Vienna, Austria
24 Murdoch Children's Research Institute. The Royal Children's Hospital, Parkville Victoria 3052 Australia
25 Department of Paediatrics, University of Melbourne Parkville Victoria 3010 Australia

Correspondence to: Mary M. Reilly
MRC Centre for Neuromuscular Diseases,
UCL Institute of Neurology, London,
WC1N 3BG, UK
E-mail: m.reilly@ucl.ac.uk

Introduction

Spinal muscular atrophy is characterized by non-length dependent loss or abnormal development of lower motor neurons. The most common form of spinal muscular atrophy is caused by recessive mutations in the *SMN1* gene on chromosome 5q (Lefebvre *et al.*, 1995). There are, however, a group of spinal muscular atrophies not caused by *SMN1* mutations (referred to as non-5q spinal muscular atrophy) and these are classified according to the clinical phenotype (Mercuri *et al.*, 2004; Reddel *et al.*, 2008). Spinal muscular atrophy, lower extremity predominant, also known as dominant congenital spinal muscular atrophy, describes a group of affected individuals with non-5q spinal muscular atrophy who have both proximal and distal weakness and wasting of lower limb muscles, but relative sparing of the upper limbs (Mercuri *et al.*, 2004; Reddel *et al.*, 2008; Oates *et al.*, 2012). Affected individuals present at birth or in the first 5 years

of life with contractures of the ankles and knees and/or congenital hip dysplasia/dislocation. Developmental motor milestones are delayed but eventually attained. Sensory symptoms and signs are typically absent. Affected individuals maintain the same degree of disability in later life suggesting a non-progressive disorder of motor neuron development.

Mutations in *DYNC1H1* were the first to be identified as a cause of spinal muscular atrophy, lower extremity predominant (OMIM: 158600) (Weedon *et al.*, 2011; Harms *et al.*, 2012; Tsurusaki *et al.*, 2012; Fiorillo *et al.*, 2014). This gene encodes the force-generating subunit of the cytoplasmic dynein motor complex, which is responsible for the transport of a large number of cellular constituents towards the minus ends of microtubules (Roberts *et al.*, 2013). More recently, mutations in the dynein adaptor protein BICD2 have been identified in a series of patients with spinal muscular atrophy, lower extremity predominant (OMIM: 615290) (Neveling *et al.*,
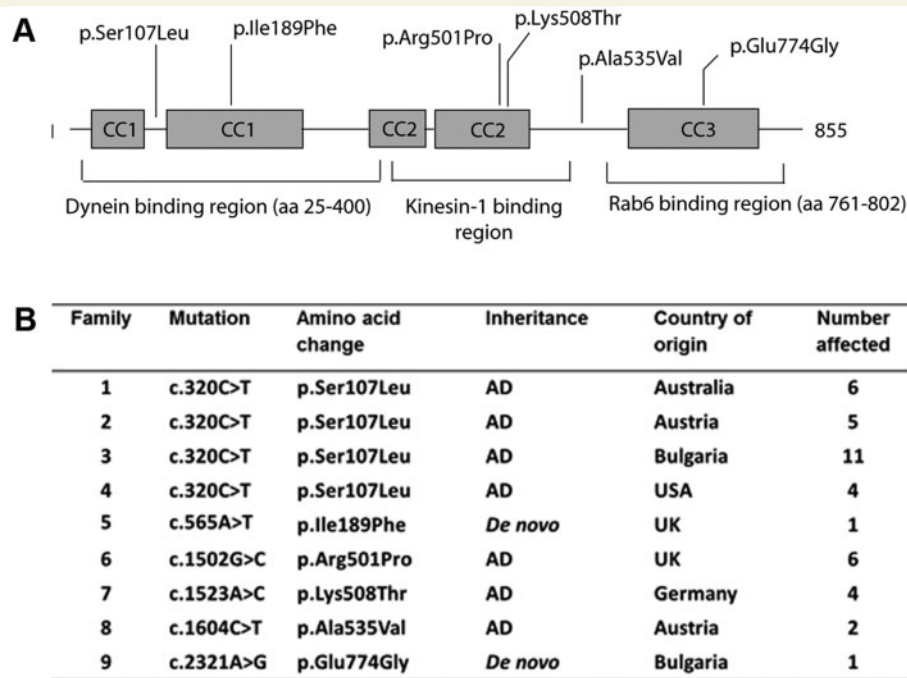
Figure 1 BICD2 mutations. (**A**) The mutations described in this paper and their positions relative to the three coiled-coil domains (CC) of the BICD2 protein. Dynein and KIF5 (kinesin 1) binding regions were defined by Splinter *et al.* (2012) and Grigoriev *et al.* (2007), respectively. The minimal Rab6-GTP binding region is based on analysis of the highly conserved *Drosophila* BicD protein (Liu *et al.*, 2013). The importance of this region for Rab6 binding is also supported by truncation analysis of human BICD2 (Bergbrede *et al.*, 2009). (**B**) Table summarizing the BICD2 mutations and families described in this paper. AD = autosomal dominant.

2013; Oates *et al.*, 2013; Peeters *et al.*, 2013; Synofzik *et al.*, 2013). A post-mortem study of one individual with spinal muscular atrophy, lower extremity predominant, subsequently found to have a p.Ser107Leu mutation in BICD2, showed features suggestive of a developmental disorder of lumbar and to a lesser extent cervical motor neurons (Oates *et al.*, 2012). BICD2 mutations have also been identified in one family with hereditary spastic paraplegia (Oates *et al.*, 2013).

The prototypic Bicaudal D (BICD) protein is from *Drosophila* and was identified as a result of a dominant mutation that causes mirror image duplications of posterior structures (bicaudal means 'two tails') because of defective transport of a mRNA that patterns the embryonic axis (Mohler and Wieschaus, 1986; Liu *et al.*, 2013). In mammals there are two BICD homologues (BICD1 and BICD2), as well as two BICD-related proteins (BICDR1 and BICDR2) (Terenzio and Schiavo, 2010). BICD and BICDR proteins link a variety of cellular cargos to the dynein motor complex, including vesicles and mRNAs (Larsen *et al.*, 2008; Dienstbier *et al.*, 2009; Bianco *et al.*, 2010; Li *et al.*, 2010; Splinter *et al.*, 2010; Hu *et al.*, 2013). BICD proteins are comprised of three putative coiled-coil (CC) domains (Fig. 1A), which lead to the formation of a homodimer. The N-terminal domain (consisting of CC1 and part of CC2) interacts with the dynein motor complex and its accessory complex dynactin (Hoogenraad *et al.*,

2001; Splinter *et al.*, 2012). The highly conserved CC3 domain mediates binding to cargos through direct interactions with cargo-associated proteins. These cargo-associated proteins include the G protein Rab6 in its GTP-bound form (Rab6-GTP) (in the case of Golgi-derived vesicles) (Matanis *et al.*, 2002), Egalitarian (Egl) and fragile X mental retardation protein (Fmr1) (in the case of mRNA) (Dienstbier *et al.*, 2009; Bianco *et al.*, 2010) and clathrin heavy chain (in the case of vesicles within the presynaptic termini of *Drosophila* neuromuscular junctions) (Li *et al.*, 2010). CC2 of human BICD2 interacts with the heavy chain of kinesin 1 (both isoforms KIF5A and KIF5B) and may coordinate the activity of this plus end-directed microtubule motor with that of dynein (Grigoriev *et al.*, 2007). Two recent studies provided compelling evidence for a model in which BICD2 promotes long distance movement of dynein by stimulating its association with the dynactin complex, thereby coupling cargo binding to activation of the motor (McKenney *et al.*, 2014; Schlager *et al.*, 2014).

In this study we describe the clinical phenotype of 32 individuals from nine families with spinal muscular atrophy, lower extremity predominant due to mutations in *BICD2*. Affected individuals had one of six mutations, which span all three coiled-coil domains of the protein. These include a previously unreported mutation, p.Ala535Val, and a likely 'hot spot' mutation,

p.Ser107Leu. We also used the recently solved crystal structure from CC3 of the *Drosophila* BicD (Liu *et al.*, 2013) to elucidate the effect of the p.Glu774Gly mutation on BICD2 cargo binding.

Materials and methods

Patient identification

Patients were recruited to this study from the inherited neuropathy and neurogenetics clinics at the National Hospital for Neurology and Neurosurgery and Great Ormond Street Hospital, London; The Children's Hospital at Westmead, Sydney, Australia; The Division of Orthopaedics, Medical University of Vienna, Austria; The Departments of Neurology and Paediatrics, Medical University-Sofia, Bulgaria; and The Department of Neurology at the University of Rochester Medical Centre and the Department of Neurology at the Connecticut Children's Medical Centre. All families included in this study had mutations in *BICD2* identified using whole exome sequencing, with or without preceding linkage analysis to identify candidate regions of interest, as previously described (Wheeler *et al.*, 2008; Li and Durbin, 2009; McKenna *et al.*, 2010; McLaren *et al.*, 2010; Zuchner *et al.*, 2011; Gonzalez *et al.*, 2013; Peeters *et al.*, 2013). All mutations identified were confirmed by Sanger sequencing and segregation analysis was performed using DNA from all available family members with the exception of Family 7 in whom DNA was only available from the proband.

This study was approved by The National Hospital for Neurology and Neurosurgery Research Ethics Committee/ Central London REC 3 09/H0716/61, the Human Ethics Committee and the Children's Hospital at Westmead, Sydney Australia #10/CHW/45; The Institutional Ethical Review Board of the University College London Institute of Child Health and Great Ormond Street Hospital in the United Kingdom (in accordance with the UK10K project ethical framework);

Clinical assessment

Affected individuals were recruited into the study if they had a confirmed mutation in *BICD2*. Thirty-two patients from nine different families were recruited. Cohort members were seen in one of the participating specialist neuromuscular centres and assessed by a senior neurologist specializing in neuromuscular diseases (M.M.R., F.M., K.N., M.A.G., D.H., I.T., I.L. or R.C.). The clinical assessment consisted of a detailed medical history and a neurological examination in all cohort members, with neurophysiological studies performed in 23/32 cohort members.

MRI

Muscle MRI was performed in six patients. Axial and coronal planes of the pelvis and lower limbs were obtained using conventional T_1-weighted spin echo sequences.

Histological analysis

A muscle biopsy was performed in two cohort members from Family 6. Autopsy-derived muscle tissue was available from a third cohort member from Family 1. Muscle histology was assessed by standard histological and histochemical stains and immunohistochemistry for fast (Families 1 and 6) and slow myosin heavy chains (Family 6 only).

Structural analysis

The structure of the minimal Rab6-binding region of *Drosophila melanogaster* BicD (from PDB file 4BL6) was modified in the program Pymol (DeLano, 2008) by manually substituting residues that are specific for the human protein. The dimer of A and D chains was used for the structural analysis in this study. Structures of human GCC185 (PDB file 3BBP) (Burguete *et al.*, 2008) and mouse RAB6IP1 (PDB file 3CWZ) (Recacha *et al.*, 2009) were derived from structures of each protein in complex with Rab6-GTP. Images of structures were generated in Pymol.

Results

Patients with mutations in BICD2 show a common phenotype

In this study we report detailed clinical data from 32 patients from nine families with mutations in *BICD2* (Figs 1 and 2). The identification of mutations in BICD2 and limited clinical description of 30 of these patients have previously been reported (Oates *et al.*, 2013; Peeters *et al.*, 2013). More detailed clinical and autopsy data from Family 1 is available in a publication which precedes the identification of the *BICD2* mutations (Oates *et al.*, 2012). The features of two individuals from Family 8, with a typical spinal muscular atrophy, lower extremity predominant phenotype, and a *BICD2* mutation (p.Ala535Val) that has not been reported previously, were also included in this study. In 31 of the 32 cohort members, from eight of the nine families, features were first noted *in utero*, at birth, or in early childhood, and consisted of lower limb-predominant non-length dependent weakness, wasting and contractures of variable severity, with reduced or absent lower limb deep tendon reflexes (i.e. a 'typical' spinal muscular atrophy, lower extremity predominant phenotype). A detailed summary of the phenotypic features is provided in Table 1.

Onset in cohort members with typical spinal muscular atrophy, lower extremity predominant features (rather than hereditary spastic paraplegia) was in the first decade and was often at or before the age of 5 years (23/31 cases). Antenatal onset characterized by reduced foetal movements, and/or breech presentation at delivery seemed to predict a more severe congenital presentation. Less severely affected individuals presented with toe walking due to Achilles tendon contractures.
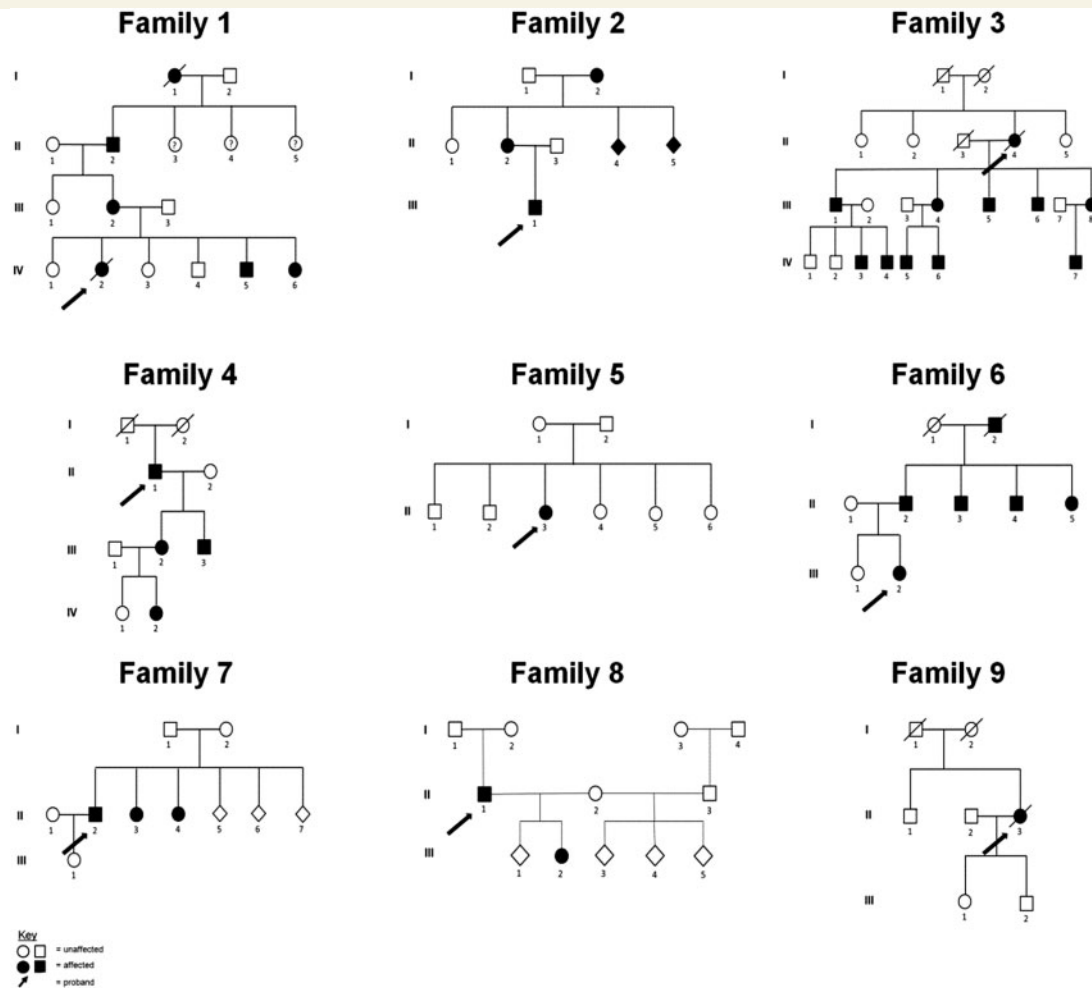
Figure 2 The pedigrees of all nine families. The pedigrees of all nine families with mutations in BICD2 described in this study.

In all affected individuals muscle weakness and wasting were most marked in the lower limbs (Fig. 3). Wasting often involved both proximal and distal leg muscles. The degree of wasting did not always correlate with the severity of weakness. For example, the affected male shown in Fig. 3C, has very severe wasting of both the thigh and lower leg but had only mild (MRC grade 4^+) weakness of ankle dorsiflexion.

Most cohort members were able to walk independently, with a minority requiring ankle foot orthoses to maintain foot positioning during ambulation. Occasionally a wheelchair was required (4/32 cohort members).

Contractures at birth or in the first decade of life were a common but not universal feature. Ankle (Achilles) contractures were the most common form and often required surgical correction, typically in the second decade of life

Congenital dysplasia of the hip with or without associated hip dislocation was present in 6/32 cohort members. Surgical correction was required in half of the cases and one-third of patients required the use of a wheelchair.

In all affected cases the phenotype was predominantly motor. Altered sensation in the hands and feet was

described in four patients (one of whom had a concurrent diagnosis of diabetes). In all cases, sensory symptoms and signs were not accompanied by abnormal sensory nerve action potentials (Table 2).

The presence of upper motor neuron features in this cohort can be used to divide patients with mutations in *BICD2* into three phenotypic categories: (i) pure lower motor neuron involvement (Families 1, 2, 3, 8 and 9); (ii) both upper and lower motor neuron involvement (Families 4, 5 and 6); and (iii) pure upper motor neuron involvement (Family 7). In Family 7, there was adult-onset of lower limb wasting, weakness and contractures, with a purely upper motor neuron phenotype consistent with the diagnosis of hereditary spastic paraplegia, rather than spinal muscular atrophy, lower extremity predominant. This individual did not, however, have an EMG examination, and it is conceivable that a lower motor neuron component may have been missed.

Scoliosis and lumbar hyperlordosis were present in 14 of 32 individuals. Scoliosis was never severe enough to warrant surgical correction. Scapular winging was present in 13/31 cohort members with typical spinal muscular

Table 1 Clinical characteristics of individuals with *BICD2* mutations

Patient Age (Sex)	Age at onset	Onset Early features	Ambulant	Pattern of muscle weakness UL prox	UL distal	LL prox	LL distal	Muscle atrophy	Contractures	CDH	Scapular winging	UMN features	Cognitive features	Additional features
1 (III.2) 38 (F)	18 months	CV, LL muscle wasting, delayed motor milestones, waddling gait	Yes Fatigues with prolonged standing or when walking over longer distances	−	−	++	++	Distal > prox LL	Bilateral asymmetrical CV, ATT (bilateral AT lengthening and cavus release surgery at age 12)	No	No	No	No	Reduced upper limb reflexes, short broad feet, medially deviated fifth toes with dysplastic toenails, chronic foot pain, lumbar hyperlordosis, symptoms suggestive of OSA
1 (IV.2) 1 (F)	Birth	TCV, unilateral CDH with dislocation, bilateral hip contractures, LL muscle wasting, delayed motor milestones	Not walking by time of death at 14 months of age	−	−	++	++	Left LL, particularly calf	Hips, knees, ATT, bilateral asymmetrical CV, Left AT/TCV surgery aged 6/12	Yes on right only (right hip surgery 6/12)	No	No	No	Reduced foetal movements in third trimester, high-arched palate, short broad feet, medially deviated fifth toes with dysplastic toenails
1 (IV.5) 9(M)	6 months	CV, LL contractures and wasting, delayed motor milestones, waddling gait	Power wheelchair for long distances (to reduce fatigue and foot pain), AFOs for shorter distances	−	−	++	++	Buttocks, prox and distal LL	Hips, knees, ATT, bilateral asymmetrical CV	No	No	No	Mild LD	Speech and swallowing difficulties suggestive of bulbar dysfunction, chronic foot pain, pectus carinatum, mild mid-thoracic scoliosis, broad feet, pes planus, lumbar hyperlordosis, positive Gowers', increased upper segment to lower segment ratio, arm span significantly longer than height, LL osteopenia, NIV from age 4 for OSA (which did not improve with removal of adenoids)
1 (IV.6) 6(F)	6 months	CV, LL muscle wasting and contractures, delayed motor milestones	Power wheelchair for longer distances (to reduce fatigue), AFOs for shorter distances	−	−	++	++	Buttocks, prox and distal LL	Hips, knees, ATT, bilateral asymmetrical CV	No	No	No	No	Asymmetrical chest wall deformity, pes planus, short broad feet, medially deviated fifth toes

(continued)

Table 1 Continued

Patient	Age (Sex)	Onset: Age at onset	Onset: Early features	Ambulant	UL prox	UL distal	LL prox	LL distal	Muscle atrophy	Contractures	CDH	Scapular winging	UMN features	Cognitive features	Additional features
2 (I.2)	77 (F)	First decade	Abnormal gait	Wheelchair since aged 69	–	+	+++	+++	LL	UK	UK	UK	UK	UK	with dysplastic toenails, lumbar hyperlordosis, positive Gowers' sign, frequent falls, increased upper segment to lower segment ratio, arm span significantly longer than height, LL osteopenia, NIV from age 4 for OSA
2 (II.2)	50 (F)	First decade	Foot deformity, waddling high stepping gait	Yes	–	–	+	++	Distal > prox LL	Foot deformity	No	No	No	No	Lumbar hyperlordosis
2 (III.2)	2 (M)	Birth	Delayed motor milestones, frequent falls, waddling gait	Yes	+	–	++	++	Shoulder girdle, prox and distal LL	UK	No	No	No	No	Lumbar hyperlordosis
3 (II.4)	48 (F)	2 years	Waddling gait	Yes	–	–	++	–	Shoulder girdle, prox LL	No	No	Yes	No	No	–
3 (III.1)	44 (M)	2 years	Delayed motor milestones, waddling gait	Yes	–	–	++	++	Shoulder girdle, prox and distal LL	No	No	Yes	No	No	Lumbar hyperlordosis
3 (III.4)	30 (F)	5 years	Waddling gait	Yes	–	–	++	–	–	No	No	No	No	No	No
3 (III.5)	24 (M)	6 years	Waddling gait	Yes	–	–	++	–	Shoulder girdle, prox and distal LL	No	No	Yes	No	No	Lumbar hyperlordosis
3 (III.6)	24 (M)	4 years	Waddling gait	Yes	–	–	++	–	Shoulder girdle, prox and distal LL	No	No	Yes	No	No	Lumbar hyperlordosis
3 (III.8)	29 (M)	4 years	Waddling gait	Yes	–	–	++	–	Shoulder girdle, prox LL	No	No	Yes	No	No	–
3 (IV.3)	6 (M)	1 year	Delayed motor milestones, waddling gait	Yes	–	–	++	–	Shoulder girdle, prox and distal LL	No	No	Yes	No	No	Bilateral deafness, lumbar hyperlordosis
3 (IV.4)	5 (M)	1 year	Delayed motor milestones, frequent falls, waddling gait	Yes	–	–	++	–	Shoulder girdle	No	No	Yes	No	LD (perinatal asphyxia)	Lumbar hyperlordosis
3 (IV.5)	6 (M)	5 years	Waddling gait	Yes	–	–	++	–	Shoulder girdle, prox LL	No	No	Yes	No	No	Lumbar hyperlordosis
3 (IV.6)	3 (M)	2 years	Waddling gait	Yes	–	–	++	–	Shoulder girdle	No	No	Yes	No	No	Lumbar hyperlordosis
3 (IV.7)	5 (M)	4 years	Waddling gait	Yes	–	–	++	–	shoulder girdle	No	No	Yes	No	No	Lumbar hyperlordosis

(continued)

Table 1 Continued

Patient Age (Sex)	Age at onset	Onset / Early features	Ambulant	Pattern of muscle weakness				Muscle atrophy	Contractures	CDH	Scapular winging	UMN features	Cognitive features	Additional features
				UL prox	UL distal	LL prox	LL distal							
4 (II.1) 54 (M)	2 years	Delayed motor milestones, abnormal gait	Yes (cane and AFOs)	+	−	++	++	Prox and distal LL	Pes cavus	No	No	No	No	Altered sensation in hands and feet, OSA
4 (III.2) 29 (F)	First decade	Waddling gait	Yes	−	−	++	−	Prox > distal LL	Pes cavus	Yes	No	Yes: brisk ankle jerks	No	Exertional and supine dyspnoea.
4 (III.3) 27 (M)	First decade	Delayed motor milestones (walking)	Yes	−	+*	++	+	LL	Pes cavus	No	No	Yes: crossed adductors, extensor plantar responses	No	—
4 (IV.2) 6 (F)	2 years	Difficulty walking	Yes	−	−	++	+	Mild LL	No	Radiological acetabular dysplasia	No	No	No	—
5 (II.3) 8 (F)	Birth	Contractures and delayed motor milestones	No Wheelchair dependent	+	−	+++	+++	Prox and distal LL	Contracture of ankles, knees (requiring surgery) and hips	Yes (Surgery)	No	Yes, brisk UL reflexes	—	—
6 (II.2) 56 (M)	4 years	Toe walking, waddling gait	Yes	−	−	−	+	Prox and distal LL	ATT (surgery aged 13)	No	No	Yes, brisk reflexes	No	—
6 (II.3) 50 (M)	Birth	Talipes, delayed walking, waddling gait	Yes	−	−	+	+	Prox and distal LL	TCV (callipers from birth)	No	No	Yes, brisk reflexes, extensor plantars	Learning difficulties	—
6 (II.4) 50 (M)	12	Toe walking, waddling gait	Yes	−	−	−	+	Prox and distal LL	Pes cavus, ATT (surgery aged 12 and 20)	No	No	Yes, brisk reflexes	No	No
6 (II.5) 50 (F)	First decade	Toe walking	Yes	−	−	−	−	No	ATT (surgery aged 6)	No	No	Yes, brisk reflexes	No	—
6 (III.2) 19 (F)	Birth	TCV and bilateral CDH. Delayed motor milestones	Intermittent wheelchair use	+/−	−	++	++	Prox and distal LL	TCV	Yes (surgery aged 6)	Yes	Yes, brisk reflexes	No	Reduced foetal movements in third trimester
7 (II.2) 69 (M)	Third decade	Abnormal gait and difficulty walking	Yes	−	−	+	+	Distal LL	Contractures of hips and knees in adulthood	No	No	Yes, brisk reflexes	No	—
8 (II.1) 45 (M)	Birth	TCV, delayed motor milestones, waddling gait	Yes	−	−	++	++	Prox and distal LL	TCV. Pes planus	Yes	No	No	No	Scoliosis
8 (III.2) 18 (F)	Birth	TCV, delayed motor milestones, waddling gait	Yes	−	−	++	++	Prox and distal LL	TCV, Pes planus	No	Yes	No	No	Scoliosis
9 (II.3) 42 (M)	First decade	Delayed motor milestones, waddling gait	Yes	−	−	++	++	Prox and distal LL	No	No	Yes	No	No	—

M = male, F = female, − = absent, + = mild, ++ = moderate, +++ = severe.
TCV = talipes calcaneovalgus; CV = non-congenital calcaneovalgus foot deformities; ATT = Achilles tendon tightening; UK = unknown; CDH = congenital dysplasia +/− additional dislocation of the hips; UL = upper limbs; LL = lower limbs; prox = proximal; AFO = ankle foot orthotics; OSA = obstructive sleep apnoea; LD = learning difficulties; UMN = upper motor neuron; NIV = non-invasive ventilation;
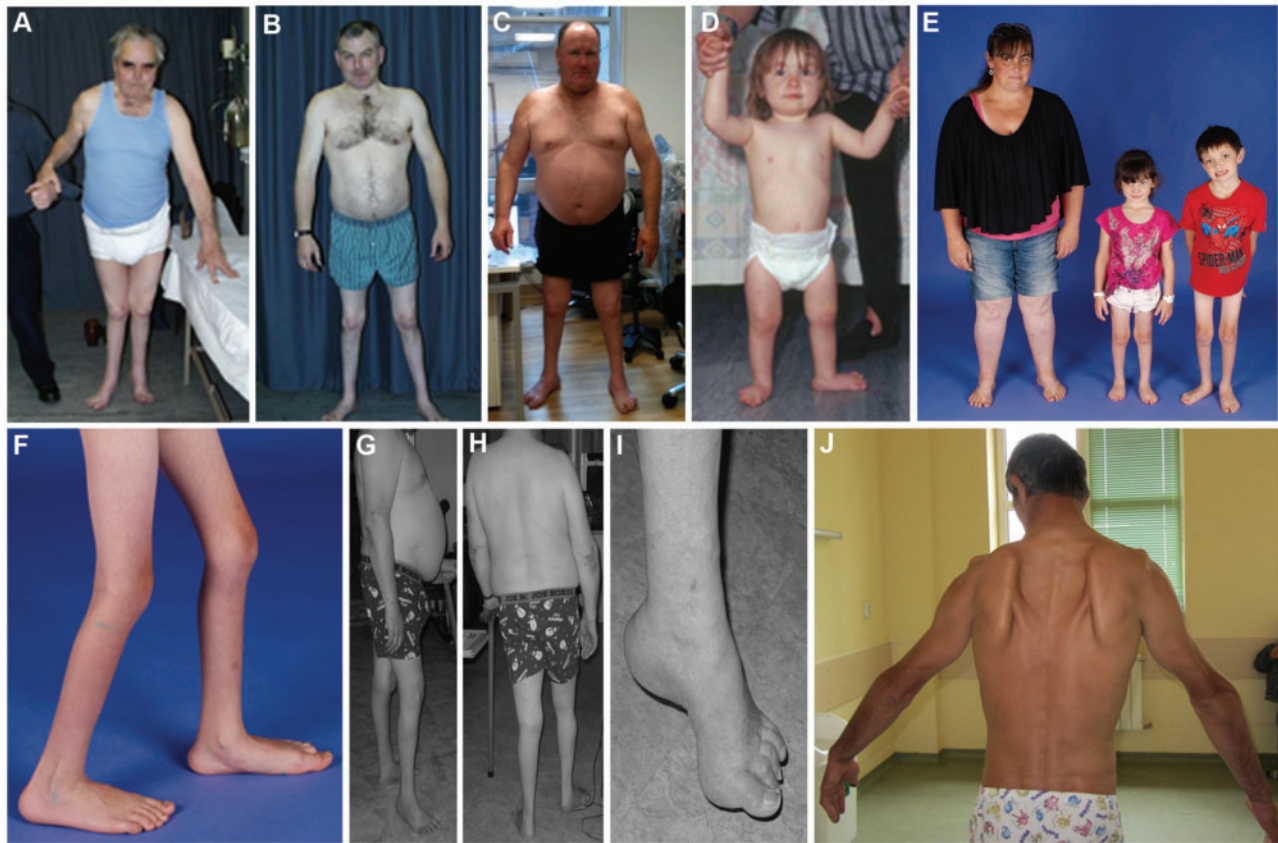
Figure 3 Clinical features of individuals with mutations in BICD2. (A–D) Images of the three affected generations of Family 6 (Patients I.2, II.2, II.3 and III.2). **(E)** Image of the two younger affected members of Family 1 and their affected mother (Patients III.2, IV.5 and IV.6). In both families lower limb muscle wasting of varying severity, with normal muscle bulk elsewhere is evident. **D** also shows the calcaneovalgus foot positioning assumed by many affected individuals when weight bearing and ambulating. **(F)** Patient IV.5 from Family 1 and **(G and H)** Patient II.1 from Family 4, demonstrating the marked wasting of both the upper and lower leg that is typically seen in more severely affected individuals. **(F and I)** The pes planus and pes cavus foot deformities that are commonly seen in this disorder. **(J)** Patient III.1 from Family 3, showing the marked scapular winging that was present in 10 of the 11 affected members of this family, and in three affected individuals from other families.

atrophy, lower extremity predominant features (including 10/11 affected members of Family 3), all of whom had proximal lower limb involvement, with or without additional distal involvement.

No cohort members had a history of epilepsy in contrast to patients with spinal muscular atrophy, lower extremity predominant due to mutations in *DYNC1H1*, where epilepsy may be a common additional feature (Vissers *et al.*, 2010; Willemsen *et al.*, 2012; Poirier *et al.*, 2013; Fiorillo *et al.*, 2014). In addition, none of the seven cohort members from Families 3, 4, 6 and 7 who underwent brain MRI nor the one patient from Family 1 at post-mortem, had evidence of malformations of cortical development. Three individuals from three separate families had learning difficulties; in one this occurred in the context of perinatal birth injury and brain MRI showed periventricular T_2 high signal consistent with hypoxic ischaemic encephalopathy. Brain MRI was performed in one of the remaining two cohort members with learning difficulties and was normal.

Neurophysiology

In the majority of affected individuals, motor nerve studies were normal with abnormalities only detected on EMG examination (Table 2). A reduction in compound muscle action potential of the common peroneal nerve was observed in 5 of 20 patients examined. Nerve conduction velocities were normal and sensory action potentials were either normal or borderline reduced. The EMG features were typical of chronic denervation and included a reduced interference pattern and the presence of large motor units with or without polyphasia. There were no signs of acute denervation such as fibrillations and positive sharp waves in any of the cohort members studied. In some affected individuals the EMG examination, although limited, was normal.

Central motor conduction studies were performed in two individuals from Family 6 and one from Family 7, all of whom had upper motor neuron signs. Cortical magnetic motor-evoked potentials to the lower limbs were prolonged in one individual from Family 7 and normal in one

Table 2 A summary of the neurophysiology of patients with mutations in BICD2

Family	Patient	Age (years)	Median motor		Ulnar motor		Peroneal motor		Tibial motor		Median sensory		Ulnar sensory		Sural sensory		Radial sensory		LL EMG
			Amp	CV	Amp	CV	Amp	CV	Amp	CV	Amp	CV	Amp	CV	Amp	CV	Amp	CV	
1	III.2	33	N	N	N	N	Borderline	N	Borderline	N	N	N	N	N	N	N	–	–	++
1	IV.5	4	N	N	–	–	N	N	N	N	–	–	–	–	N	N	–	–	++
2	II.2	50	–	–	–	–	2.0	46.0	11.9	48.0	–	–	–	–	9.0	58.0	–	–	+
3	III.1	44	15.1	60.5	–	–	2.4	43.5	–	–	25.8	61.6	–	–	14.2	52.7	–	–	+
3	III.4	30	–	–	–	–	–	–	–	–	–	–	–	–	–	–	–	–	+
3	IV.3	6	11.6	57	–	–	10.1	54.8	–	–	10.4	51.3	–	–	N	N	–	–	+
3	IV.4	5	–	–	–	–	6.1	58.3	–	–	10.0	49.7	–	–	–	–	–	–	+
3	IV.5	6	–	–	–	–	7.7	55.1	–	–	–	–	–	–	–	–	–	–	+
4	II.1	55	9.35	50.9	8.67	50.0	1.85	–	–	48.6	24	–	9.7	–	14	–	–	–	+
4	III.1	27	10.39	57	–	–	8.45	48.2	15.16	48.6	43.7	–	42.9	–	29.9	–	–	–	+
4	III.2	27	11.7	55.8	10.1	57.6	2.3	–	–	–	46.3	–	32.2	–	–	–	47.2	–	N^
4	IV.2	11/12	N	N	N	N	N	N	–	–	N	N	–	–	–	–	–	–	+
5	II.3	3	N	N	–	–	Absent	–	–	–	–	–	–	–	–	–	–	–	+
6	I.2	13	10.1	61	–	–	5.7	42	2.2	–	32	56.5	–	–	21	44.5	–	–	+
6	II.1	55	4.7	57	11.2	60	7.9	43	–	–	10	46	7	57.5	8	38.5	–	–	+
6	II.2	54	8.8	52	10.3	58	5.1	39	2.8	–	5	43.5	10	56	12	46	67	67	+
6	II.3	53	4.1	53	14.8	59	4.4	46	11.0	–	11	47	5	54	28	52.5	23	61.5	+
6	II.4	50	2.8*	–	6.1*	–	9.5	47	–	–	13	47	6	63	12	59	45	68.5	N^
7	II.2	69	–	–	–	–	–	–	N	N	–	–	–	–	N	N	–	–	–
8	II.1	45	13.5	58.0	–	–	5.0	47.0	–	–	20.0	56.0	–	–	5.0	67.0	–	–	–
8	III.2	18	15.2	56.0	9.1	–	12.0	45.3	7.8	–	43.5	65.7	40	62.5	19.2	48.6	–	–	–
9	II.3	42	14.5	56.0	–	–	11.2	45.0	N	N	N	N	N	N	N	N	ND	ND	+

*submaximal stimulation.

N = normal; – = not done; Amp = amplitude (µV); CV = conduction velocity (m/s); LL = lower limbs; + = chronic denervation and re-innervation (reduced interference pattern, large polyphasic motor units); ++ = large amplitude non-polyphasic motor units action potentials; ^ = limited study.

individual from Family 6. In the other subject from Family 6, cortical magnetic motor-evoked potentials were normal but motor-evoked potentials using spinal magnetic stimulation of the ventral roots were borderline prolonged.

Muscle MRI

MRI of the muscles at the level of the thigh and calf was performed in six individuals from four families. The severity of fat replacement of muscle varied in proportion to the clinical severity but conformed to a common pattern with selective involvement and sparing of individual muscles. A striking feature was the presence of small foci of normal muscle within fatty muscle tissue (Fig. 4).

At the level of the thigh there was variable fatty replacement of the rectus femoris, vastus lateralis, vastus intermedius, semi-membranosus, long head of biceps and sartorius with sparing and in some cases hypertrophy of the adductor and semi-tendinosus muscles. At the level of the calf there was fatty replacement of the tibialis anterior and gastrocnemius muscles with sparing of the peroneal muscles. This is a very similar pattern to that seen in patients with spinal muscular atrophy, lower extremity predominant due to mutations in *DYNC1H1* (Fig. 4).

Brain and spine MRI

MRI of the brain and spine was undertaken in four members of Families 5 and 6 (with typical spinal muscular atrophy, lower extremity predominant features) and in one member of Family 7 (with a diagnosis of hereditary spastic paraplegia). In all cases imaging was normal.

Muscle histology

Muscle histopathology findings were variable in the three affected individuals for whom muscle was available (Fig. 5). A quadriceps needle biopsy taken from Patient II.2 of Family 6 at 39 years showed marked variation in fibre size (5–150 μm) with increased internal nuclei, increased connective tissue, whorled and split fibres and frequent mini-core like lesions with absent oxidative enzymes. Fibre typing with NADH-TR was indistinct and the majority of fibres expressed slow myosin. Fast myosin was present in a few small fibres (data not shown). Patient III.2 from the same family had a muscle biopsy at 3 years from an unspecified site and showed mild variability of fibre size with type I fibre uniformity across all fascicles (based on NADH staining). Both biopsies were interpreted to be myopathic. In the affected individual in whom denervation was the predominant feature at autopsy (Patient IV.2 from Family 1), atrophic fibres were generally positive for fast myosin. Fast myosin negative fibres appeared to be numerous, and were predominant in many areas. For all assessed muscles, groups of fast myosin negative fibres were more common than groups of fast myosin positive fibres, and fast myosin negative fibres were

typically normal in size, or hypertrophied. The overall picture was in keeping with chronic denervation with reinnervation. The diaphragm was histopathologically normal (data not shown). A description of the autopsy-based muscle and spinal cord histopathology has previously been published (Oates *et al.*, 2012).

Prognosis

Disease progression was extremely slow or static, particularly once affected individuals reached adulthood. This is in contrast to many other forms of spinal muscular atrophy (including 5q spinal muscular atrophy) and distal hereditary motor neuropathy which typically follow a progressive course (Rossor *et al.*, 2012), but is akin to spinal muscular atrophy, lower extremity predominant due to mutations in *DYNC1H1*. While the lower motor neuron weakness was slowly or non-progressive, upper motor neuron signs when present became more prominent with increasing age.

The p.Ser107Leu substitution may represent a mutation hot spot for BICD2

The c.320C>T (p.Ser107Leu) mutation is in a CpG dinucleotide and most likely represents a methylcytosine-deamination mutation. Four of the nine families in this cohort have this mutation (Families 1, 2, 3 and 4). We have previously shown that Families 1 and 2 from Australia and Austria, respectively, share an 8-SNP (single nucleotide polymorphism) haplotype with a background frequency in the European population of ~2% suggesting that the p.Ser107Leu mutation in these two families arose from a relatively recent founder mutation rather than arising *de novo* in both families (Oates *et al.*, 2013). Due to difficulties in establishing phase of relevant local single nucleotide polymorphisms we were unable to determine whether Family 4 also shares a common haplotype. The absence of the p.Ser107Leu mutation in the first generation of Family 3 confirms that the mutation in this family has arisen independently from the mutation in other families. The p.Ser107Leu mutation may therefore represent a 'hot spot' mutation.

Structural insights into how the p.Glu774Gly mutation in BICD2 disrupts Rab6 binding

The p.Glu774Gly mutation in CC3 of BICD2 has only been described in a sporadic case of spinal muscular atrophy, lower extremity predominant in whom segregation could not be confirmed in the parents (Peeters *et al.*, 2013). Co-precipitation studies in tissue culture cells showed that this mutation results in strongly reduced association between BICD2 and Rab6a, compared to the level observed for wild-type BICD2 (Peeters *et al.*, 2013). Consistent with
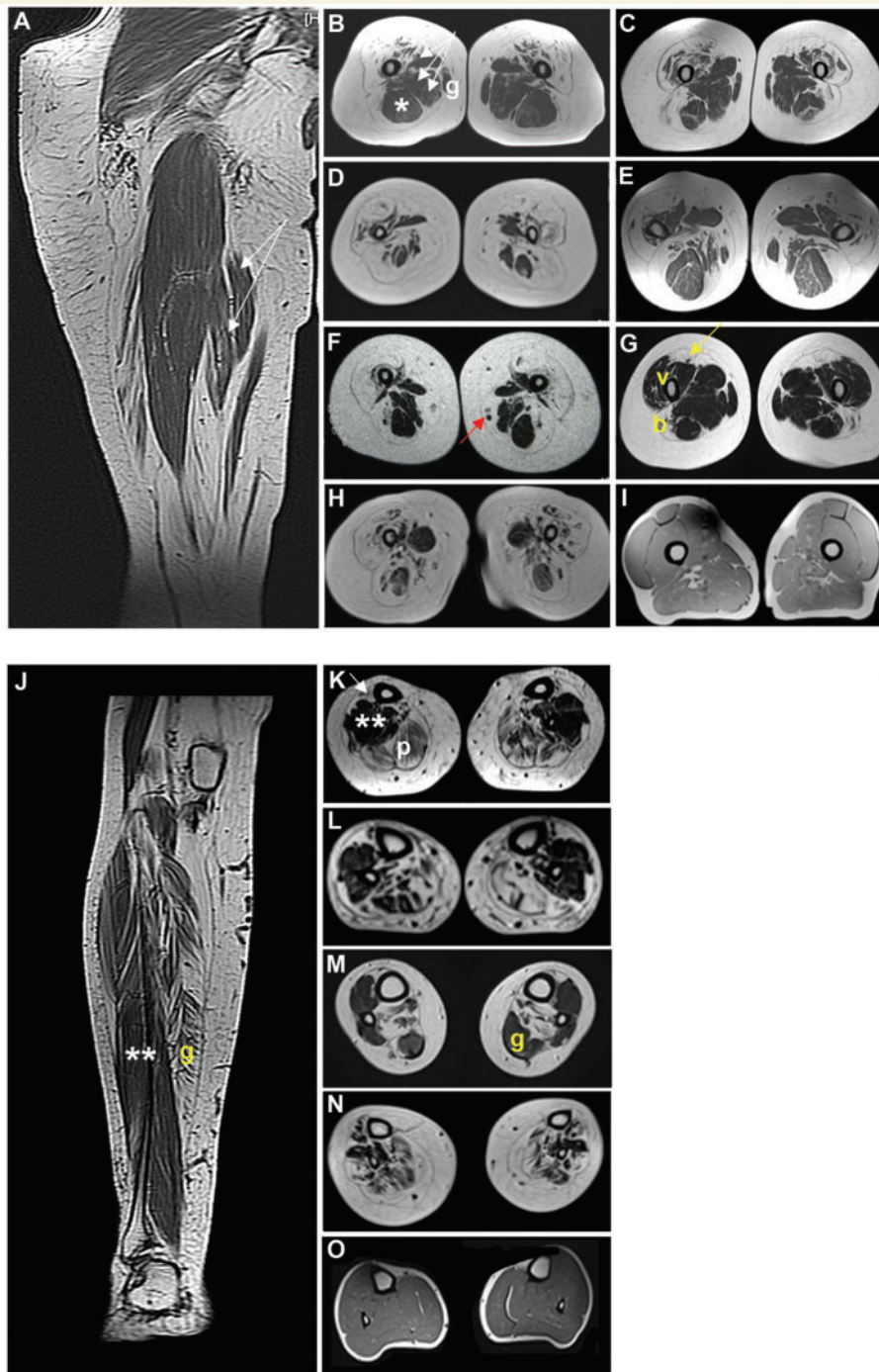
Figure 4 Lower limb muscle MRI findings in individuals with *BICD2*- and *DYNC1H1*-spinal muscular atrophy, lower extremity predominant. T$_1$-weighted coronal and axial muscle magnetic resonance images of the lower limb in individuals with spinal muscular atrophy, lower extremity predominant due to mutations in *BICD2* (**A–G** and **J–M**), with lower limb images from an individual with *DYNC1H1*-spinal muscular atrophy, lower extremity predominant (p.Arg598Cys mutation) (**H** and **N**) and an unaffected (normal) individual (**I** and **O**) shown for comparison. (**A–I**) Images of the upper leg, including axial upper thigh images (**B–I**). (**J–O**) Images of the lower leg, including axial lower calf images (**K–O**). The MRI panels correspond to the following cohort members; **A**, **B**, **J** and **K** = Family 1, Patient III.2 (at age 32 years); **C** = Family 2 Patient III.1 (at age 50 years); **D** = Family 5, Patient II.3 (at age 8 years); **E** and **L** = Family 6, Patient II.3 (at age 52 years); **F** = Family 6, Patient III.2 (at age 10 years); **G** and **M** = Family 8, Patient III.2 (at age 45 years); **H** and **N** = *DYNC1H1*-spinal muscular atrophy, lower extremity predominant case (at age 20 years); **I** and **O** = normal individual (at age 33 years). MRI of the upper leg shows a common pattern of muscle involvement in individuals with mutations in *BICD2* and *DYNC1H1* with variable fat replacement of the muscles of the anterolateral thigh but relative sparing with or without relative hypertrophy of the semitendinosus muscle (white asterisk, **B**), the medially placed adductor muscles (adductor longus, brevis and magnus; white arrows in **B**), and gracilis ('g' in **B**). In milder cases, vastus lateralis and vastus intermedius (lower case yellow 'v' in **G**) are less involved than in more severe cases (e.g. **D**), however rectus femoris (yellow arrow in **G**) and long head of biceps femoris ('b' in **G**) remain markedly involved.

(continued)

these findings, p.Glu774Gly also strongly reduced the enrichment of BICD2 with Rab6a-positive structures, as assessed by fluorescence microscopy of cultured cells. The strong reduction in cargo association caused by p.Glu774Gly and the fact that the clinical phenotype is so similar to the phenotype of other individuals with familial *BICD2* mutations (Peeters *et al.*, 2013) (Table 1), provides strong evidence that this is the causative disease mutation in the affected individual. However, it was not clear how this mutation results in altered BICD2 cargo binding.

To further explore this issue we exploited the recently solved 2.2 angstrom crystal structure from a region of CC3 of the *Drosophila* BicD protein [amino acids (aa) 656–745; PDB code 4BL6], which contains the minimal Rab6-GTP binding domain (Liu *et al.*, 2013). This is the only high resolution BICD protein structure currently available. The minimal Rab6-GTP binding region is comprised of aa 702–743 of the *Drosophila* protein (Liu *et al.*, 2013), which corresponds to aa 761–802 of human BICD2. These sequences are 71.4% identical and 90.5% similar (i.e. accounting for substitutions of amino acids with similar properties) between *Drosophila* BicD and human BICD2. The structure of the *Drosophila* protein can therefore be used to model with confidence the structure formed by the human sequence.

Glu774 (Glu715 in the *Drosophila* protein) occupies a surface-exposed position on the coiled-coil dimer (a 'g' position in the heptad repeat that is the building block of the coiled-coil structure) (Lupas and Gruber, 2005) (Fig. 6A). This amino acid is positioned close to other evolutionarily conserved residues that were shown to be critical for binding of the *Drosophila* BicD to Rab6-GTP (Liu *et al.*, 2013) (Fig. 6A and B). Thus, the side chain of Glu774 could be involved in directly contacting Rab6-GTP. Consistent with this notion, comparison of the electrostatic surface potential of this region of BICD2 with that of Rab6-binding regions of two other proteins, the coiled-coil protein GCC185 (Burguete *et al.*, 2008) and RAB6IP1 (Recacha *et al.*, 2009), reveals the presence in all three cases of glutamate side chains, which are large and negatively charged, flanking a region with positively charged and hydrophobic (i.e. neutral) residues. This arrangement may be required to form a functional Rab6-binding site. In the case of GCC185 and RabIP1, for which crystal structures are available in complex with Rab6-GTP, glutamate residues mediate direct interactions with the Rab protein (Burguete *et al.*, 2008; Recacha *et al.*, 2009). A similar function of Glu774 in BICD2 could therefore account for reduced Rab6-GTP binding when this residue is mutated to glycine, which has a minimal side chain.

Discussion

In this study we report the features of the largest single cohort of patients with mutations in *BICD2*, and identify a common phenotype that allows for focused genetic testing and interpretation of whole exome or genome data.

Onset of clinical features in members of this cohort with spinal muscular atrophy, lower extremity predominant (rather than hereditary spastic paraplegia), and in most previously published cases (Neveling *et al.*, 2013) has typically been within the first decade of life. In the most severely affected individuals, onset is *in utero*. One exception to this rule is a recently described three generation spinal muscular atrophy, lower extremity predominant kindred (with typical clinical and MRI features), segregating for a *BICD2* mutation that results in an amino acid change (p.Arg747Cys) within the third coiled-coil domain of BICD2. While the youngest member of this kindred developed symptoms in childhood, her mother and grandfather did not notice symptoms until their 30s and early 40s (Synofzik *et al.*, 2013). The later age of onset is similar to that for members of Family 7 (with a p.Lys508Thr mutation and a purely upper motor neuron phenotype) and suggests that in a minority of affected individuals the disorder may present after childhood.

In all members of this cohort the lower limbs were disproportionately affected and the degree of wasting was often out of proportion to the degree of weakness. This is in keeping with the phenotype of patients with spinal muscular atrophy, lower extremity predominant due to missense mutations in the cytoplasmic dynein heavy chain, DYNC1H1 (Weedon *et al.*, 2011; Harms *et al.*, 2012; Tsurusaki *et al.*, 2012; Fiorillo *et al.*, 2014). The marked degree of lower limb muscle involvement was also evident on muscle MRI, which shows a characteristic pattern of muscle fat replacement and selective hypertrophy similar to that seen in patients with *DYNC1H1* mutations.

Despite the lower extremity predominance, mild upper limb involvement such as scapular winging was present in a subset of cohort members. Scapular winging has also been reported in patients with spinal muscular atrophy, lower extremity predominant due to mutations in *DYNC1H1* (Harms *et al.*, 2012) and, when present, may be a useful additional diagnostic clue to this group of disorders.

Figure 4 Continued
A striking feature is the presence of small foci of normal muscle within denervated muscle (red arrow in **F**). MRI of the lower leg also shows a common pattern of muscle involvement in both *BICD2* and *DYNC1H1* cases. The posterior compartment muscles ('p' in **K**), including the gastrocnemius and soleus are typically involved, with sparing with or without relative hypertrophy of the muscles of the lateral compartment (extensor digitorum longus and hallucis, peroneus longus and brevis, double asterisk in **K**). Tibialis anterior is also markedly involved (arrow, **K**), even in mildly affected individuals. (**M**) Relative sparing of gastrocnemius is sometimes seen in more mildly affected individuals (yellow 'g' in **M**, shown more severely involved with yellow 'g' in **J**).
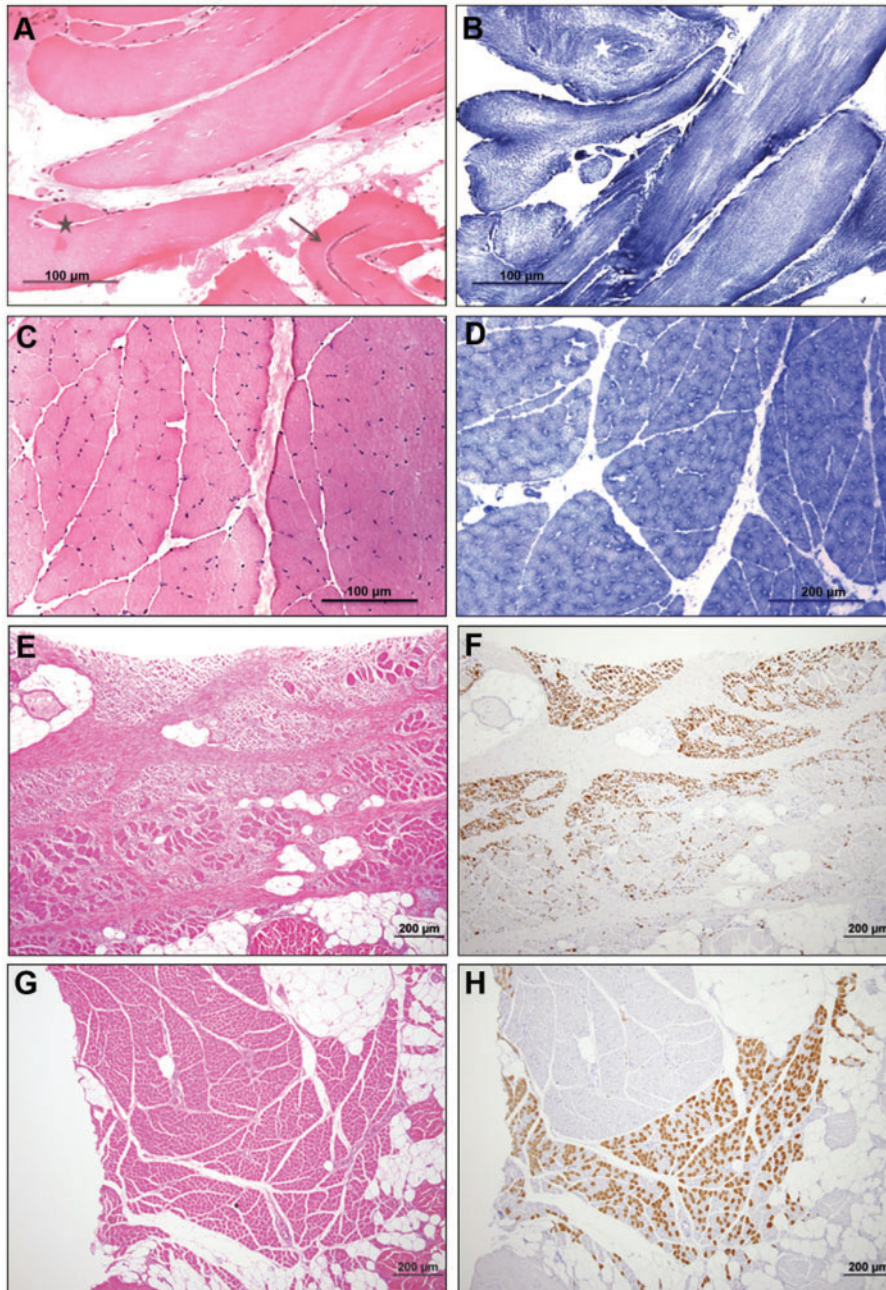
Figure 5 Muscle pathology in *BICD2*-spinal muscular atrophy, lower extremity predominant. Muscle pathology findings in *BICD2*-spinal muscular atrophy, lower extremity predominant are highly variable, and may show minimal change, pseudomyopathic features, and/or typical neuropathic features including fibre type grouping with or without atrophy. (**A**) Pseudomyopathic changes with extreme fibre size variation, fibre splitting (black star), slightly increased connective tissue, and internal nuclei (black arrow) in an obliquely orientated quadriceps needle biopsy performed at 39 years of age from an affected member of Family 6 (Patient II.2) (haematoxylin and eosin). (**B**) NADH-TR oxidative enzyme staining of the same muscle biopsy shows disturbed internal architecture including whorled fibres (**B**, white star) and frequent core-like lesions of variable size (white arrow). (**C** and **D**) Images of a muscle biopsy from another affected individual from Family 6 (Patient III.2), taken at 3 years of age from an unspecified muscle during corrective hip surgery showing little abnormality except variation in the number of fibres per fascicle (**C**, haematoxylin and eosin), and marked predominance/uniformity of type I fibres with staining for NADH-TR (**D**). (**E** and **F**) Post-mortem sections of vastus lateralis from Family 1 Patient IV.2, aged 14 months, stained with haematoxylin and eosin (**E**) and the serial area immunolabelled for fast myosin (**F**) showing increased interstitial fat, increased perimysial and endomysial connective tissue (**E**), and grouped atrophy of predominantly fast myosin-positive fibres (**F**). Hypertrophic fibres typically did not stain for fast myosin, suggesting they expressed slow myosin, but hybrid fibres were not assessed. Less severely involved lower limb muscles, such as the peroneus (Family 1 Patient IV.2) show areas of fibre-type grouping of normal-sized fibres (**G**, haematoxylin and eosin; **H**, fast myosin).
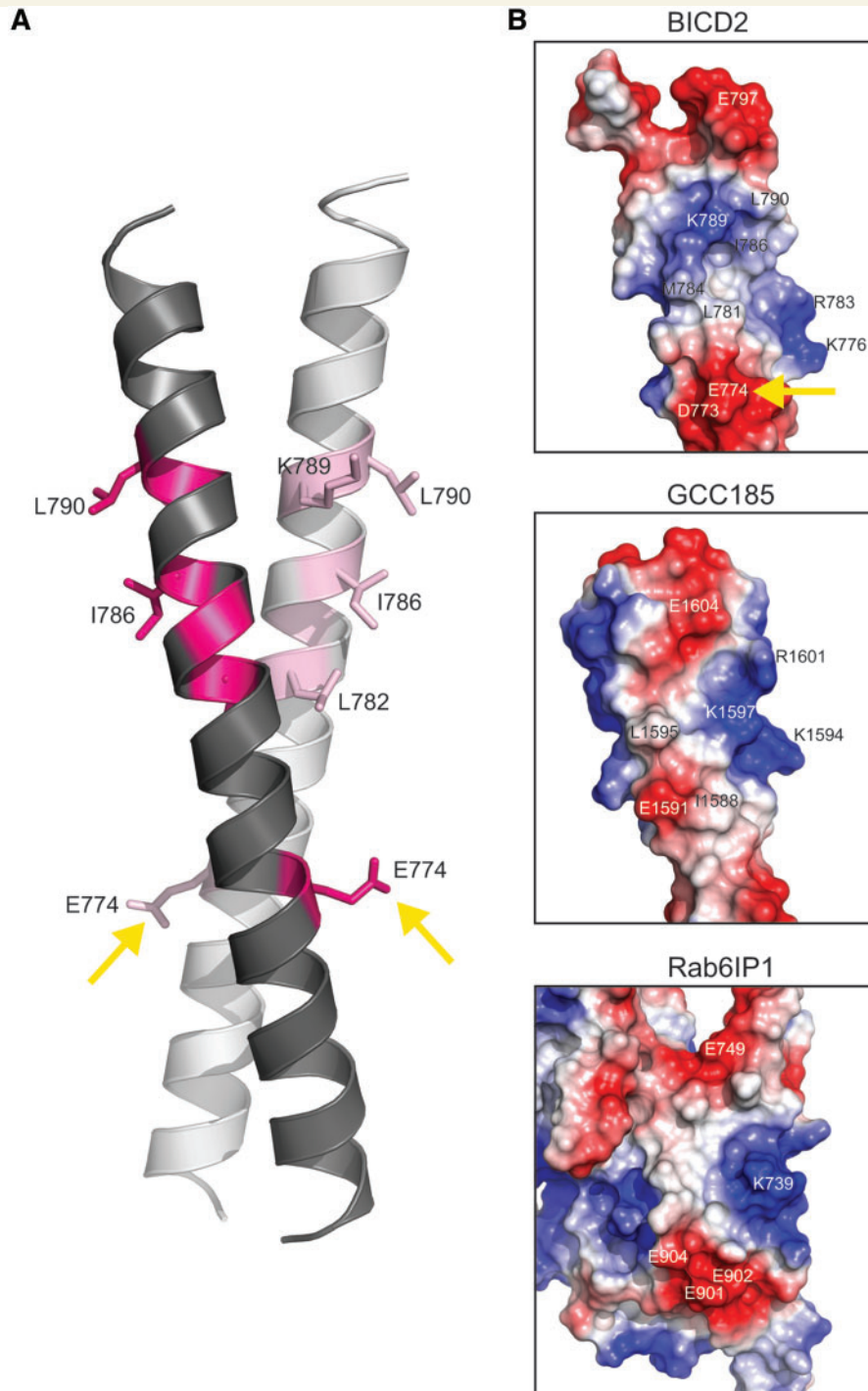
Figure 6 Structural analysis of the position of Glu774 in BICD2. (**A**) Representation of the structure of the minimal Rab6-binding region of BICD2 (aa761–802), modelled on the crystal structure from CC3 of the highly conserved *Drosophila* BicD (PDB 4BL6). Side chain group position of Glu774 in each polypeptide chain of the BICD2 coiled coil is shown (yellow arrows) with respect to those of residues that are known to be critical for Rab6-GTP binding to CC3 of the *Drosophila* protein (Liu *et al.*, 2013). The orientation of the structure is selected to show the surface-exposed position of Glu774. Note that there are two identical binding sites for Rab6-GTP on opposing faces of the coiled-coil dimer (Liu *et al.*, 2013). Each binding site is likely to be comprised of side chains from both polypeptide chains, which is the case for the interaction of the GCC185 coiled coil with Rab6-GTP (Burguete *et al.*, 2008). All side chains shown are identical in the *Drosophila* proteins except Ile786, which is a Val in fruit fly BicD. Ile and Val both have hydrophobic, aliphatic side groups and their properties are therefore very similar. (**B**) Electrostatic surface potential of structures of the minimal Rab6-binding regions of BICD2, GCC185 and Rab6IP, with putative Rab6-binding sites face-on. All three structures contain regions of negative charge (red) flanking regions that are hydrophobic (white) or positively charged (blue). GCC185 and Rab6IP contain negatively charged Glu residues that can directly contact Rab6-GTP (Burguete *et al.*, 2008; Recacha *et al.*, 2009). Glu774 of BICD2 (labelled with a yellow arrow) may serve a similar function in binding to cargo associated proteins, thus explaining reduced Rab6 binding for

(continued)

Whilst the motor phenotype associated with *BICD2* mutations is similar to that seen in individuals with *DYNC1H1* mutations, malformations of cortical development and epilepsy, that are sometimes present in individuals with *DYNC1H1* mutations, were not a feature in our *BICD2* cohort. Overall these findings suggest that mutations in *BICD2* predominantly affect dynein function in motor neurons and that the effect of mutant DYNC1H1 on cortical development and neuronal migration is largely independent of BICD2. This notion is compatible with the finding that the dynein motor uses multiple adaptors, including different BICD family members (Kardon and Vale, 2009; Terenzio and Schiavo, 2010) to associate with different cargos.

Mutations in *TRPV4* have also been identified in a large kindred with typical spinal muscular atrophy, lower extremity predominant features (Fleury and Hageman, 1985; Auer-Grumbach *et al.*, 2010), and in a small number of additional individuals with 'congenital distal spinal muscular atrophy' (Astrea *et al.*, 2012). *TRPV4* encodes a transient receptor potential cation channel, and mutations in *TRPV4* are associated with a variety of clinical phenotypes including scapuloperoneal spinal muscular atrophy, Charcot-Marie-Tooth disease Type 2C, distal hereditary motor neuropathy (Auer-Grumbach *et al.*, 2010; Deng *et al.*, 2010; Landoure *et al.*, 2010), and a range of skeletal dysplasias (Nishimura *et al.*, 2012). The clinical and MRI features of *TRPV4*-spinal muscular atrophy, lower extremity predominant are subtly different to *DYNC1H1*- and *BICD2*-spinal muscular atrophy, lower extremity predominant e.g. equinovarus rather than calcaneovalgus foot deformities (Fleury and Hageman, 1985), and lower limb MRI does not show sparing of the thigh adductors, and semtitendinosus, but instead shows sparing of biceps femoris (Astrea *et al.*, 2012). These differences suggest a different pathophysiology for TRPV4-related spinal muscular atrophy, lower extremity predominant.

Whilst the phenotype of early-onset, lower extremity predominant wasting and weakness is common to most patients with mutations in *BICD2*, there was considerable heterogeneity in terms of the severity of the phenotype. The reason for the phenotypic heterogeneity is unknown but has important implications for genetic counselling.

The variable muscle pathology findings highlight the difficulty in diagnosing long-standing denervation in small biopsies, as it is not always easy to distinguish myopathic fibre type predominance from extensive fibre type grouping. A range of secondary architectural abnormalities including structural lesions such as mini-cores and cores and fibro-fatty infiltration, so called 'pseudomyopathic' features, may accrue over time in chronically denervated muscle confounding the diagnosis as seen in the biopsy from Patient II.2, Family 6. The preferential atrophy of type II (fast) fibres suggests that the pathogenesis of this disease may favour preservation of motor neurons innervating slow fibres; however, this pattern is also observed in other chronic neurogenic conditions including 5q spinal muscular atrophy.

It is clear from our cohort that there is involvement of upper motor neurons in a proportion of patients with mutations in *BICD2*. Although two individuals with mutations in CC1 displayed upper motor neuron features, upper motor neuron involvement appears to be more common in families with mutations in CC2. The mutations in CC2 are found in the region that can interact with kinesin 1 (Grigoriev *et al.*, 2007) but outside the region that is sufficient to bind the dynein-dynactin complex (Splinter *et al.*, 2012) (Fig. 1). It is therefore possible that altered interactions of BICD2 with kinesin 1 are associated with upper motor neuron defects. Compatible with this notion, mutations of the kinesin 1 protein KIF5A are associated with familial hereditary spastic paraplegia (Reid *et al.*, 2002).

At the time of writing, three mutations have been identified in CC3 of BICD2: p.Thr703Met, p.Arg747Cys and p.Glu774Gly (Neveling *et al.*, 2013; Peeters *et al.*, 2013; Synofzik *et al.*, 2013). Only the latter two residues are contained within the region of *Drosophila* BicD that was crystallized for structure determination (Liu *et al.*, 2013). Based on the *Drosophila* structure, Arg747 of BICD2 is predicted to be in a region of highly unusual coiled-coil structure that regulates dynein recruitment in response to cargo binding to more C-terminal sequences (Liu *et al.*, 2013). However, the consequence of an Arg to Cys change at this position is unclear. In contrast, our current analysis of the location of Glu774 within the modelled structure of human BICD2 suggests that the side chain could directly interact with Rab6-GTP. This would account for the reduced Rab6 binding observed in a previous study of the p.Glu774Gly mutation (Peeters *et al.*, 2013). Recent evidence suggests that the same or overlapping features on BICD proteins that mediate Rab6-GTP binding can also mediate interactions with other cargo-associated proteins (Liu *et al.*, 2013). Thus, Glu744Gly may compromise binding to proteins other than Rab6-GTP and this may contribute to the pathophysiology in the individual with this mutation. Indeed, no evidence was found for an involvement of Rab6 in the loss-of-function phenotype of *Drosophila* BicD at the neuromuscular junction (Li *et al.*, 2010). This phenotype, which is characterized by selective paralysis of posterior segments at larval stages and reduced neurotransmission, appears instead to be associated with

Figure 6 Continued

p.Glu774Gly. Note that the region of the GCC185 coiled-coil that directly contacts Rab6-GTP is comprised of at least 16 amino acids on each chain (Burguete *et al.*, 2008), equivalent to the distance between Glu774 and Leu790 of BICD2. In each structure a subset of residues is labelled for orientation purposes (the choice of white and black lettering is purely to increase visibility against the background colour). The single letter amino acid code is used in the figure panels.

defects in recycling of clathrin-associated synaptic vesicles (Li *et al.*, 2010).

In summary we have analysed the phenotypic features in the largest BICD2 cohort to be described and have confirmed that mutations in BICD2 typically cause early-onset non-length dependent lower limb predominant weakness, wasting and contractures, with a relatively static clinical course.

Overall, the features are consistent with *BICD2*-disease being a 'developmental' form of spinal muscular atrophy—caused by a pathological process that preferentially affects the primary development and/or early survival of a specific subpopulation of lower motor neurons. The clinical similarity between *BICD2*- and *DYNC1H1*- spinal muscular atrophy, lower extremity predominant has highlighted dynein-dynactin trafficking as a key cellular pathway in motor neuron patterning, primary development, and survival, and a potential therapeutic target for motor neuron disorders in general.

Acknowledgements

Funding

References

Astrea G, Brisca G, Fiorillo C, Valle M, Tosetti M, Bruno C, et al. Muscle MRI in TRPV4-related congenital distal SMA. Neurology 2012; 78: 364–5.

Auer-Grumbach M, Olschewski A, Papic L, Kremer H, McEntagart ME, Uhrig S, et al. Alterations in the ankyrin domain of TRPV4 cause congenital distal SMA, scapuloperoneal SMA and HMSN2C. Nat Genet 2010; 42: 160–4.

Bergbrede T, Chuky N, Schoebel S, Blankenfeldt W, Geyer M, Fuchs E, et al. Biophysical analysis of the interaction of Rab6a GTPase with its effector domains. J Biol Chem 2009; 284: 2628–35.

Bianco A, Dienstbier M, Salter HK, Gatto G, Bullock SL. Bicaudal-D regulates fragile X mental retardation protein levels, motility, and function during neuronal morphogenesis. Curr Biol 2010; 20: 1487–92.

Burguete AS, Fenn TD, Brunger AT, Pfeffer SR. Rab and Arl GTPase family members cooperate in the localization of the golgin GCC185. Cell 2008; 132: 286–98.

DeLano WL. The PyMOL molecular graphic system. Palo Alto, CA: Scientific LLC; 2008.

Deng HX, Klein CJ, Yan J, Shi Y, Wu Y, Fecto F, et al. Scapuloperoneal spinal muscular atrophy and CMT2C are allelic disorders caused by alterations in TRPV4. Nat Genet 2010; 42: 165–9.

Dienstbier M, Boehl F, Li X, Bullock SL. Egalitarian is a selective RNA-binding protein linking mRNA localization signals to the dynein motor. Genes Dev 2009; 23: 1546–58.

Fiorillo C, Moro F, Yi J, Weil S, Brisca G, Astrea G, et al. Novel dynein DYNC1H1 neck and motor domain mutations link distal spinal muscular atrophy and abnormal cortical development. Hum Mutat 2014; 35: 298–302.

Fleury P, Hageman G. A dominantly inherited lower motor neuron disorder presenting at birth with associated arthrogryposis. J Neurol Neurosurg Psychiatry 1985; 48: 1037–48.

Gonzalez MA, Lebrigio RF, Van Booven D, Ulloa RH, Powell E, Speziani F, et al. GEnomes Management Application (GEM.app): a new software tool for large-scale collaborative genome analysis. Hum Mutat 2013; 34: 842–6.

Grigoriev I, Splinter D, Keijzer N, Wulf PS, Demmers J, Ohtsuka T, et al. Rab6 regulates transport and targeting of exocytotic carriers. Dev Cell 2007; 13: 305–14.

Harms MB, Ori-McKenney KM, Scoto M, Tuck EP, Bell S, Ma D, et al. Mutations in the tail domain of DYNC1H1 cause dominant spinal muscular atrophy. Neurology 2012; 78: 1714–20.

Hoogenraad CC, Akhmanova A, Howell SA, Dortland BR, De Zeeuw CI, Willemsen R, et al. Mammalian Golgi-associated Bicaudal-D2 functions in the dynein-dynactin pathway by interacting with these complexes. EMBO J 2001; 20: 4041–54.

Hu DJ, Baffet AD, Nayak T, Akhmanova A, Doye V, Vallee RB. Dynein recruitment to nuclear pores activates apical nuclear migration and mitotic entry in brain progenitor cells. Cell 2013; 154: 1300–13.

Kardon JR, Vale RD. Regulators of the cytoplasmic dynein motor. Nat Rev Mol Cell Biol 2009; 10: 854–65.

Landoure G, Zdebik AA, Martinez TL, Burnett BG, Stanescu HC, Inada H, et al. Mutations in TRPV4 cause Charcot-Marie-Tooth disease type 2C. Nat Genet 2010; 42: 170–4.

Larsen KS, Xu J, Cermelli S, Shu Z, Gross SP. BicaudalD actively regulates microtubule motor activity in lipid droplet transport. PloS One 2008; 3: e3763.

Lefebvre S, Burglen L, Reboullet S, Clermont O, Burlet P, Viollet L, et al. Identification and characterization of a spinal muscular atrophy-determining gene. Cell 1995; 80: 155–65.

Li H, Durbin R. Fast and accurate short read alignment with Burrows-Wheeler transform. Bioinformatics 2009; 25: 1754–60.

Li X, Kuromi H, Briggs L, Green DB, Rocha JJ, Sweeney ST, et al. Bicaudal-D binds clathrin heavy chain to promote its transport and augments synaptic vesicle recycling. EMBO J 2010; 29: 992–1006.

Liu Y, Salter HK, Holding AN, Johnson CM, Stephens E, Lukavsky PJ, et al. Bicaudal-D uses a parallel, homodimeric coiled coil with heterotypic registry to coordinate recruitment of cargos to dynein. Genes Dev 2013; 27: 1233–46.

Lupas AN, Gruber M. The structure of alpha-helical coiled coils. Adv Protein Chem 2005; 70: 37–78.

Matanis T, Akhmanova A, Wulf P, Del Nery E, Weide T, Stepanova T, et al. Bicaudal-D regulates COPI-independent Golgi-ER transport by recruiting the dynein-dynactin motor complex. Nat Cell Biol 2002; 4: 986–92.

McKenna A, Hanna M, Banks E, Sivachenko A, Cibulskis K, Kernytsky A, et al. The genome analysis toolkit: a MapReduce framework for analyzing next-generation DNA sequencing data. Genome Res 2010; 20: 1297–303.

McKenney RJ, Huynh W, Tanenbaum ME, Bhabha G, Vale RD. Activation of cytoplasmic dynein motility by dynactin-cargo adapter complexes. Science 2014; 345: 337–41.

McLaren W, Pritchard B, Rios D, Chen Y, Flicek P, Cunningham F. Deriving the consequences of genomic variants with the Ensembl API and SNP effect predictor. Bioinformatics 2010; 26: 2069–70.

Mercuri E, Messina S, Kinali M, Cini C, Longman C, Battini R, et al. Congenital form of spinal muscular atrophy predominantly affecting the lower limbs: a clinical and muscle MRI study. Neuromuscul Disord 2004; 14: 125–9.

Mohler J, Wieschaus EF. Dominant maternal-effect mutations of Drosophila melanogaster causing the production of double-abdomen embryos. Genetics 1986; 112: 803–22.

Neveling K, Martinez-Carrera LA, Holker I, Heister A, Verrips A, Hosseini-Barkooie SM, et al. Mutations in BICD2, which encodes a golgin and important motor adaptor, cause congenital autosomal-dominant spinal muscular atrophy. Am J Hum Genet 2013; 92: 946–54.

Nishimura G, Lausch E, Savarirayan R, Shiba M, Spranger J, Zabel B, et al. TRPV4-associated skeletal dysplasias. Am J Med Genet C 2012; 160C: 190–204.

Oates EC, Reddel S, Rodriguez ML, Gandolfo LC, Bahlo M, Hawke SH, et al. Autosomal dominant congenital spinal muscular atrophy: a true form of spinal muscular atrophy caused by early loss of anterior horn cells. Brain 2012; 135 (Pt 6): 1714–23.

Oates EC, Rossor AM, Hafezparast M, Gonzalez M, Speziani F, Macarthur DG, et al. Mutations in BICD2 cause dominant congenital spinal muscular atrophy and hereditary spastic paraplegia. Am J Hum Genet 2013; 92: 965–73.

Peeters K, Litvinenko I, Asselbergh B, Almeida-Souza L, Chamova T, Geuens T, et al. Molecular defects in the motor adaptor BICD2 cause proximal spinal muscular atrophy with autosomal-dominant inheritance. Am J Hum Genet 2013; 92: 955–64.

Poirier K, Lebrun N, Broix L, Tian G, Saillour Y, Boscheron C, et al. Mutations in TUBG1, DYNC1H1, KIF5C and KIF2A cause malformations of cortical development and microcephaly. Nat Genet 2013; 45: 639–47.

Recacha R, Boulet A, Jollivet F, Monier S, Houdusse A, Goud B, et al. Structural basis for recruitment of Rab6-interacting protein 1 to Golgi via a RUN domain. Structure 2009; 17: 21–30.

Reddel S, Ouvrier RA, Nicholson G, Dierick I, Irobi J, Timmerman V, et al. Autosomal dominant congenital spinal muscular atrophy–a possible developmental deficiency of motor neurones? Neuromuscul Disord 2008; 18: 530–5.

Reid E, Kloos M, Ashley-Koch A, Hughes L, Bevan S, Svenson IK, et al. A kinesin heavy chain (KIF5A) mutation in hereditary spastic paraplegia (SPG10). Am J Hum Genet 2002; 71: 1189–94.

Roberts AJ, Kon T, Knight PJ, Sutoh K, Burgess SA. Functions and mechanics of dynein motor proteins. Nat Rev Mol Cell Biol 2013; 14: 713–26.

Rossor AM, Kalmar B, Greensmith L, Reilly MM. The distal hereditary motor neuropathies. J Neurol Neurosurg Psychiatry 2012; 83: 6–14.

Schlager MA, Hoang HT, Urnavicius L, Bullock SL, Carter AP. *In vitro* reconstitution of a highly processive recombinant human dynein complex. EMBO J 2014; 33: 1855–68.

Splinter D, Razafsky DS, Schlager MA, Serra-Marques A, Grigoriev I, Demmers J, et al. BICD2, dynactin, and LIS1 cooperate in regulating dynein recruitment to cellular structures. Mol Biol Cell 2012; 23: 4226–41.

Splinter D, Tanenbaum ME, Lindqvist A, Jaarsma D, Flotho A, Yu KL, et al. Bicaudal D2, dynein, and kinesin-1 associate with nuclear pore complexes and regulate centrosome and nuclear positioning during mitotic entry. PLoS Biol 2010; 8: e1000350.

Synofzik M, Martinez-Carrera LA, Lindig T, Schols L, Wirth B. Dominant spinal muscular atrophy due to BICD2: a novel mutation refines the phenotype. J Neurol Neurosurg Psychiatry 2013; 85: 590–2.

Terenzio M, Schiavo G. The more, the better: the BICD family gets bigger. EMBO J 2010; 29: 1625–6.

Tsurusaki Y, Saitoh S, Tomizawa K, Sudo A, Asahina N, Shiraishi H, et al. A DYNC1H1 mutation causes a dominant spinal muscular atrophy with lower extremity predominance. Neurogenetics 2012; 13: 327–32.

Vissers LE, de Ligt J, Gilissen C, Janssen I, Steehouwer M, de Vries P, et al. A *de novo* paradigm for mental retardation. Nat Genet 2010; 42: 1109–12.

Weedon MN, Hastings R, Caswell R, Xie W, Paszkiewicz K, Antoniadi T, et al. Exome sequencing identifies a DYNC1H1 mutation in a large pedigree with dominant axonal Charcot-Marie-Tooth disease. Am J Hum Genet 2011; 89: 308–12.

Wheeler DA, Srinivasan M, Egholm M, Shen Y, Chen L, McGuire A, et al. The complete genome of an individual by massively parallel DNA sequencing. Nature 2008; 452: 872–6.

Willemsen MH, Vissers LE, Willemsen MA, van Bon BW, Kroes T, de Ligt J, et al. Mutations in DYNC1H1 cause severe intellectual disability with neuronal migration defects. J Med Genet 2012; 49: 179–83.

Zuchner S, Dallman J, Wen R, Beecham G, Naj A, Farooq A, et al. Whole-exome sequencing links a variant in DHDDS to retinitis pigmentosa. Am J Hum Genet 2011; 88: 201–6.